Quantum Electronics **34** (12) 1127 – 1132 (2004) ©2004 Kvantovaya Elektronika and Turpion Ltd

PACS numbers: 42.55.Px; 78.20.Jq
DOI: 10.1070/QE2004v034n12ABEH002788

Electro-optical properties of UV-emitting InGaN heterostructures considering injection-induced conductivity

P.G. Eliseev, J. Lee, M. Osinski

Abstract. **Some radiative and electric properties of heterostructures based on semiconductor nitrides emitting in the visible and UV regions are considered. The following anomalous properties of UV-emitting heterostructures are studied: the low-temperature emission quenching, a strong non-ideality of $I-V$ curves, and the increase in the slope of these characteristics upon cooling. The anomalous emission quenching is especially typical for $\sim$3-nm thick single-quantum-well structures, but it is absent in a 50-nm thick double heterostructure. It seems that this difference is caused by the fact that the capture of carriers at the levels in quantum wells slows down upon cooling, and a 'through' injection of carriers occurs into the opposite emitter layer. In addition, electrons injected into the p region reduce its resistance. The consideration of the injection-induced conductivity in the passive layer allows us to explain satisfactorily the electric anomalies.**

Keywords: *heterostructures, injection, electro-optical properties of heterostructures.*

1. Introduction

Quantum-well InGaN heterostructures are used in light-emitting diodes (LEDs) emitting in the short-wavelength range between 360 and 520 nm and also in lasers emitting between 380 and 420 nm [1 – 4]. A number of electro-optical properties of these structures are not finally explained so far. The experimental results presented in papers [5 – 7], including $I-V$ curves and watt – ampere characteristics, show that luminescence of quantum-well InGaN LEDs is strongly quenched at low temperatures, whereas emission of most of the III – V group semiconductors increases, as a rule, upon cooling. In [5], the recombination balance was studied in green InGaN LEDs and it was shown that, although the electric conduction of the LED was preserved down to 10 K, the emission intensity considerably decreased. Because the energy barriers between the InGaN quantum well and emitters are rather high, it is difficult to imagine that this decrease can occur at low temperatures due to a thermally-induced escape of carriers from the quantum well to emitters.

It was assumed that another mechanism takes place in this case, namely, the appearance of a 'ballistic' flow of carriers through the active medium without their capture in the quantum well. Indeed, the mean free path of carriers increases upon cooling, and when it becomes greater than the quantum-well width, a part of injected carriers penetrates to the opposite emitter and thus recombines outside the quantum well. It is natural that in the opposite emitter, say, in the p region, such electrons are pulled in by the electric field, as the electrons thermally activated from the quantum well. Simply, the number of 'ballistic' electrons at low temperature proves to be much greater than that of thermally activated ones. These variants of the behaviour can be distinguished by performing comparative measurements with other structures based on InGaN.

It was shown [7] that when the UV emission of InGaN LEDs decreases upon cooling, the LEDs continue emit in the blue region, so that the emission mechanism changes at the temperature 170 – 200 K and the emission band shifts approximately by 300 meV to the red. The blue emission at 450 nm is related to the recombination in the p region, in particular, in the p-GaN layer heavily doped with magnesium. Such doping leads to the formation of deep centres emitting in the blue region [8]. In additional studies of photoluminescence of diode heterostructures, both the UV and blue bands were observed; however, the blue band disappeared when the p-GaN layer was etched out [7]. It was concluded that at low temperature the injected electrons, which have flied in a ballistic flow through the active region, penetrate into the p region, where they produce blue emission. This mechanism reduces the intensity of emission through the quantum well. It is interesting that the emission intensity is higher in a structure with five quantum wells, which is explained by a higher probability of the electron capture in one of the quantum wells.

Another property of UV heterostructures, which was described in [7], is that the formal analysis of $I-V$ curves leads to a very high non-ideality factor n, which is equal to ~ 8 at room temperature and increases up to ~ 80 at liquid nitrogen temperature. It is assumed usually that a large value of this factor indicates to the tunnelling transfer mechanism of injected carriers [9]. In this case, one can expect that the value of nkT is virtually independent of temperature. However, the value of nkT in UV hetero-

P.G. Eliseev P.N. Lebedev Physics Institute, Russian Academy of Sciences, Leninskii prosp. 53, 119991 Moscow, Russia; present address: Center for High Technology Materials, University of New Mexico, Albuquerque, NM, USA; e-mail: eliseev@chtm.unm.edu;
J. Lee, M. Osinski Center for High Technology Materials, University of New Mexico, Albuquerque, NM, USA

Received 8 July 2004
Kvantovaya Elektronika **34** (12) 1127 – 1132 (2004)
Translated by M.N. Sapozhnikov

structures strongly increases upon cooling, approximately from 200 meV at room temperature up to 620 meV at 90 K ($n \sim 80$), which contradicts to the tunnelling model.

In this paper, we consider and compare the properties of InGaN structures emitting in the UV and visible regions. We take into account that the injection of electrons into the p region changes the conductivity of passive regions of the diode. The concept of *the injection-induced conductivity* allows us to explain the properties of the $I-V$ curve, in particular, a great formal value of n.

2. Samples

Let us compare emitting structures described in [7] with InGaN-based diodes studied in detail. The first type of structures is the experimental samples of UV-emitting heterostructures with InGaN quantum wells [one (SQW) or five (MQW)] located between two undoped AlGaInN layers of thickness 6 nm each, which are in turn placed between n-AlGaN:Si and p-AlGaN:Mg emitter layers. More detailed data are presented in [7]. The second type of structures is highly efficient commercial LEDs (Nichia Chemical Industry) with a quantum well [5] emitting in the green region. The 2.5–3.5-nm thick active layer in such diodes is located between larger-gap n-GaN : Si and p-AlGaN : Mg emitter layers. The third type of structures considered here is also commercial double heterostructure LEDs (Nichia Chemical Industry) [1, 2] with the 50-nm thick InGaN : Si, Zn active layer placed between n-AlGaN : Si and p-AlGaN:Mg emitter layers. In this case, carriers of both signs are injected into the 'bulk' active layer, and the radiative recombination in the blue spectral region occurs through deep centres produced by the Zn impurity. The parameters of samples are presented in Table 1.

3. Results and discussion

3.1 Temperature dependence of the radiative efficiency

Figure 1 shows the temperature dependences of the relative external efficiency normalised to the maximal value for a given current. The efficiency of the UV quantum-well structure is very low at low temperature, it achieves a maximum near room temperature and then decreases with increasing temperature. However, the efficiency of the double heterostructure emitting in the blue region weakly depends on temperature, which confirms the assumption that the problem can be reduced to the capture of carriers in the active region, which is a 'bottleneck' of the radiative mechanism in the quantum well. By contrast, such a problem does not exist in other double heterostructures because the thickness of the active region in them is much greater. As for the power decrease at temperatures above room temperature, this effect is typical for semiconductors and is caused by the increase in the role of nonradiative recombination (including all recombination types outside the active region due to leakage of all types). Note that InGaN LEDs are distinguished by their high thermal stability among other LEDs based on the III–V group compounds and operate up to the temperature ~ 600 K.

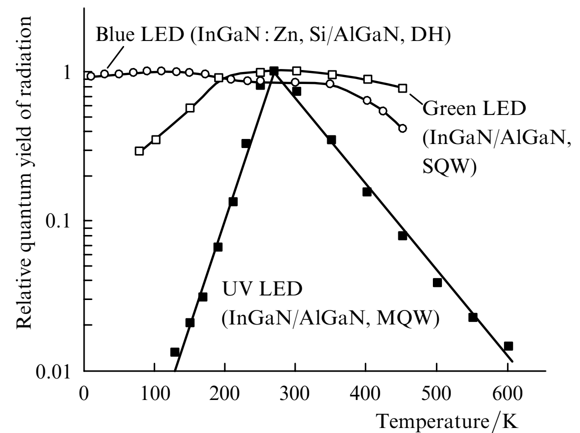

Figure 1. Temperature dependences of the relative external efficiency (normalised to the maximum value) for InGaN-based emitting structures of three types: (■) UV structure with five quantum wells; (□) green LED with a quantum well; (○) blue LED (see Table 1).

Figure 1 also shows the temperature dependence of the efficiency of a green LED based on the InGaN quantum well. One can see that the radiation efficiency also decreases at low temperatures, however, this decrease is not so strong as for the UV LED. The difference between these quantum-well structures is that the UV structure has a symmetric profile of the composition in AlGaN emitters and AlGaInN barriers, whereas the quantum well in the green LED is located between n-GaN and p-AlGaN emitters. Therefore, in the latter case there exists an additional potential barrier for electrons from the p side, which is caused by the difference between the conduction bands in GaN and AlGaN and is approximately estimated as 250 meV. Hence, the probability of the ballistic transport of electrons to the p side is substantially lower, and the radiative efficiency decreases upon cooling not so strongly an in symmetric UV LEDs.

Let us discuss the mean free path Λ of electrons with respect to their capture in a quantum well. We will take the following facts into account: this mean free path at room temperature is not sufficiently large (~ 3 nm) for the capture in one quantum well to dominate; however, the transport to the p side produces some blue emission from the p-GaN layer. In multilayer quantum-well structures (five wells with a total thickness of 15 nm) and double heterostructures (with the well thickness of 50 nm), electrons are captured almost completely. Therefore, 3 nm $\leqslant \Lambda$ (300 K) $<$ 15 nm.

Table 1. Some parameters of LEDs studied in the paper.

Diode type	Structure type	Active layer composition	Active layer thickness/nm	Wavelength at 300 K/nm	External quantum efficiency (%)	References
UV LED	SQW	$In_{0.05}Ga_{0.95}N$	3	375	–	
UV LED	MQW	$In_{0.05}Ga_{0.95}N$	3×5	375	–	
Green LED	SQW	$In_{0.22}Ga_{0.78}N$	2.5–3.5	520	5–6	[3, 5]
Blue LED	DH	$In_{0.06}Ga_{0.94}N$:Zn, Si	50	420	$\sim$2.4	[1]

The radiation from quantum wells in multilayer structures disappears at temperatures 170 – 200 K, which gives Λ (200 K) $\sim$ 15 nm. At a lower temperature, 15 nm < Λ (100 K) < 50 nm. The upper limit is determined by the fact that in double heterostructures at low temperatures the problem of capture is probably absent and the ballistic transport is not revealed. Because quantum wells in InGaN structures are usually comparatively thin, the problem of capture in them at low temperatures can be quite important. This problem is partially removed in multilayer structures with many quantum wells. This was probably used in the development of emitting structures. For example, the number of quantum wells in the active region in the InGaN lasers is 10 – 20 [4]. At lower temperatures, these structures do not produce lasing because the rate of electron capture in the quantum well is not high enough. The low-temperature capture regime noticeably improves in the case of an asymmetric shaping of the band structure: a larger-gap material is located on the *p* side rather than on the *n* side. This is confirmed by a higher efficiency of green LEDs at low temperatures.

We can use the calculations of the electron capture in the GaN quantum well [10] for comparison. The time of electron capture by the levels of a quantum well upon weak pumping is $\sim$ 0.8 ps, and this time decreases down to 20 fs with increasing pump power. According to our estimate, the free path with respect to the electron capture changes in this case from $\sim$ 200 to $\sim$ 5 nm, i.e., within a broad range. However, this calculated value proves to be larger than the width of a single quantum well in our case ($\sim$ 3 nm). This suggests that the ballistic transport is quite probable. Note that the calculation takes self-consistently into account a piezoelectric field in a strained quantum well. Unlike this, under the assumption of plane bands, the electron capture time proves to be much longer ($\sim$ 3.6 ps), and, hence, the free path time increases.

As for the injection of electrons to the *p* side, this process was considered in paper [11] for the InGaN/GaN/AlGaN laser structure with five quantum wells and a separate confinement. In the case of a large bias (lasing regime, the current density 20 kA cm^{-2}), a strong through injection of electrons occurs to the *p* side, which is favoured by an insufficient hole injection (because of a small mobility of holes) and by a small barrier height between the InGaN quantum well and GaN barrier layer. As a result, the recombination rate in the *p* side proved to be comparable with that in quantum wells. It was also pointed out in [11] that bright LEDs operating at density currents lower than 1 kA cm^{-2} do not suffer from this type of electron leakage. Under other conditions being identical, the calculated through injection increases with temperature (and explains quenching above room temperature). Note that the diffusion-drift model neglects the ballistic transport. Nevertheless, this model predicts a strong pulling of electrons into the *p* region.

3.2 Volt – ampere characteristics

Figure 2 shows the $I-V$ curve of the UV diode. These dependences are characterised by a rather high voltage compared to the expected contact voltage difference, which hardly exceeds 3.8 eV in the $p-n$ junction in AlGaN. For example, for the current 100 mA at temperature 300 K, the excess voltage is 0.9 V, and assuming that this drop occurs in the *p*-AlGaN layer, we obtain that the electric field strength in this layer will be 90 kV cm^{-1}. This means that electrons will be pulled by this field, and the free path time of the drift will be $\sim$ 0.2 ps for the 100-nm thick layer. Therefore, recombination in this layer is negligible and most of the pulled in electrons will reach the *p*-GaN region. Upon cooling down to 90 K, the strength of the pulling field increases up to $\sim$ 240 kV cm^{-1}. It seems that at low temperature and great field strength, field emission can occur from the quantum well to the *p* side. One should bear in mind that the resistance of this layer is sensitive to the value of the total current flowing through the structure and, therefore, it is no longer linear ('ohmic').

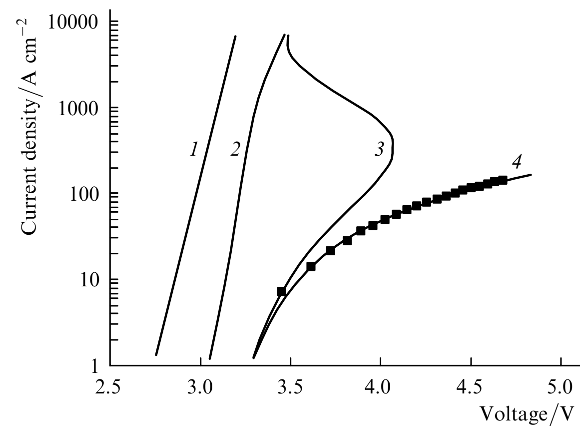

Figure 2. Experimental $I-V$ curve (■) taking into account the injection-induced conductivity: (*1*) straight line corresponding to the $I-V$ curve parameter $\varepsilon = 51$ meV ($n = 2$); (*2*) calculated dependence of the recombination current on the Fermi voltage at room temperature; (*3*) S-shaped dependence of the recombination current on the Fermi voltage taking into account the voltage drop on the *p*-AlGaN layer (effect of the injection-induced conductivity); (*4*) same as (*3*), taking into account the voltage drop on a linear series resistance.

The diode voltage $U(I)$ is usually separated into the linear and nonlinear components, the nonlinear component corresponding to the voltage across the $p-n$ junction,

$$U(I) = IR_s + \frac{\varepsilon}{e}\ln\frac{I}{I_s}, \quad (1)$$

where U is the voltage across the diode; R_s is the 'ohmic' resistance connected in series with the $p-n$ junction; ε is an $I-V$ curve parameter of the $p-n$ junction (below, the slope parameter), which is often denoted as nkT; and I_s is the saturation current (saturation upon the reverse bias, which is not related to the saturation effects in the laser). The fitting of the experimental data for UV diodes with the help of expression (1) [7] gave extremely high values of ε (620 meV at 90 K, which corresponds to $n = 80$). It is difficult to explain this value, the more so as the effective value of ε [i.e., the value obtained by formal fitting by (1)] strongly increases with decreasing temperature, which contradicts to both the tunnelling mechanism [9] and classical diffusion model [12].

The curves in Fig. 2 are constructed using the model taking into account the injection-induced conductivity and the fact that the resistance of passive regions, in our case the *p* region, in the presence of the flow of carriers into it decreases under the action of injection and, therefore,

cannot be considered as a linear resistance, but should be included into the nonlinear part of the $I-V$ curve. The fitting is shown in more detail in Fig. 2 for the experimental data obtained for the UV diode at room temperature. Here, the initial calculated curve (*2*) corresponds to the recombination current in the active region as a function of the Fermi voltage $V_F = \Delta F/e$ (ΔF is the difference of the Fermi quasi-levels). Its mean slope is close to the exponential with the parameter $\varepsilon = 2kT$ [curve (*1*)]. Curve (*3*) was obtained taking into account the voltage drop across the resistance of the *p*-AlGaN emitter layer of thickness 100 nm. It is S-shaped because this addition decreases at a high forward bias due to the induced conductivity. In a given case, we take into account only the contribution from excess electrons to the conductivity of the *p*-AlGaN layer. The concentration of these electrons was calculated using the 'quasi-equilibrium' hypothesis, i.e., assuming that the electron concentration in this layer is determined by the same Fermi quasi-level as in the quantum well. Curve (*4*) takes into account the voltage drop across the linear part of the series resistance and can be used as the $I-V$ curve of the diode.

4. Injection-induced conductivity

4.1 Resistance of the injection-sensitive layer

Because we concluded that the electrons injected into the InGaN-based quantum-well structures penetrate to a great extent into the *p* region, it is necessary to take into account the dependence of the resistance on current, which causes the nonlinear behaviour of the passive part of the diode. It seems that the near-contact heavily doped *p*-GaN layer is weakly injection-sensitive because it has the initially low resistance. The most sensitive is the *p*-AlGaN emitter layer of thickness 100 nm in which the conductivity is comparatively low and is subjected to a partial freezing at low temperature. Moreover, this layer, being a thin potential barrier between the narrower-gap layers, proves to be depleted of carriers, so that its conductivity can strongly depend on the electron injection. Let us introduce the resistance $R(I)$ of this sensitive layer, which depends on the concentration $N(I)$ of excess carriers

$$R(I) = \frac{d}{e\mu(1+b)N(I)S}, \tag{2}$$

where d is the layer thickness; μ is the electron mobility; b is the hole-to-electron mobility ratio; and S is the diode area. Although the calculated resistance at room temperature and the nominal equilibrium concentration of holes $\sim 10^{17}$ cm^{-3} is comparatively small, we assume that due to the depletion of carriers this resistance $R(0)$ in the absence of injection is 40 – 50 Ω, and in the case of strong injection, it decreases to the negligible value. The voltage drop across this resistance increases with increasing current, passes through a maximum and then decreases, which can result in a considerable change in the diode $I-V$ curve compared to the $I-V$ curve of the $p-n$ junction, and sometimes in the S-shaped $I-V$ curve, which is observed upon double injection.

It was shown above that the resistance $R(I)$ can be calculated with the help of the quasi-equilibrium model, in which the Fermi level is assumed the same for electrons in the quantum well and emitter layer. However, this model is not always valid, and the distribution of electrons and holes should be found in the general case by solving the kinetic problem.

The 'quasi-equilibrium' hypothesis can be probably realised at room temperature when recombination occurs predominantly in the quantum well rather than in barriers. It seems that this approach cannot be applied at lower temperatures. The matter is that, when the probability of capture in the quantum well is not high enough, the population functions of the energy levels in the quantum well and barrier cannot be described by the same Fermi level. According to calculations [10] performed for the GaN quantum well of width 5 nm located between the AlGaN barriers, the real difference between the electronic Fermi quasi-levels for the quantum well and barrier can be 100 – 200 meV upon threshold pumping and temperature 300 K. The quantitative development of a more detailed kinetic model for this system is complicated due to the absence of data on the mean free path of electrons with respect to their capture in the InGaN quantum well and on reemission of electrons from the well. Because of this, we used the phenomenological approach at low temperatures (see Section 4.2). This approach postulates the presence of an injection-sensitive layer in which the concentration of excess carriers is a simple function of the pump current. Note that such a sensitive layer can be a depleted layer on the *p* side. This layer was calculated for laser double heterostructures in paper [13].

4.2 Phenomenological model

Figure 3 shows the dependence of the concentration of excess electrons in the emitter *p* layer in the quasi-equilibrium model on the pump current density. The calculated concentrations are well described in a broad density range by the power dependence with the exponent from unity to 0.85. At current densities above 1 kA cm^{-2}, the dependence becomes stronger because of a considerable degeneracy in the quantum well. The concentration N in the sensitive layer can be written in a more general form as

$$N(I) = N_0\left[1 + (I/I_0)^m\right], \tag{3}$$

where N_0 is the equilibrium concentration; and I_0 and m are fitting parameters. The quantity I_0 is the current at which the concentration is doubled compared to the 'dark' value N_0. The resistance of the sensitive layer is

$$R(I) = \frac{R_0}{1 + (I/I_0)^m}, \tag{4}$$

and the diode $I-V$ curve can be written in the form

$$U(I) = IR_s + \frac{\varepsilon}{e}\ln\frac{I}{I_s} + \frac{IR_0}{1 + (I/I_0)^m}, \tag{5}$$

where the last term is a correction to the injection-induced conductivity. This phenomenological approach does not use $N(I)$ in the explicit form but postulates that $N(I)$ is an increasing power function, which satisfactorily approximates the real dependence at least within the pump current region where the resistance of the sensitive layer still plays a certain role.

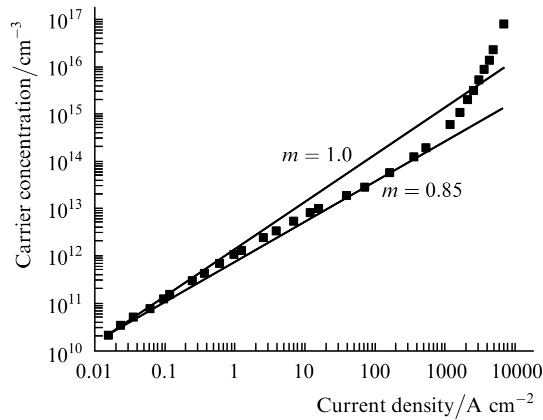

Figure 3. Calculated dependence of the carrier concentration in the p-AlGaN emitter layer on the pump current density in the quasi-equilibrium model at room temperature (■); solid straight lines are power dependences with exponents $m = 1.0$ and 0.85.

Fitting by expression (2) gives satisfactory results (Fig. 4). The fitting parameters are presented in Table 2. Because their number is comparatively large, their values can be varied within some limits without sacrificing the fitting. As for the parameter ε, it can be varied in a broad range, i.e., the result of fitting weakly depends on its value. The assumption about a simple diffusion mechanism of injection gives $\varepsilon \sim 2kT$, which was used in the calculation of the curves in Fig. 4. Therefore, the use of this model eliminates the problem of the anomalously large value of ε and of its anomalous temperature dependence: the real $I-V$ curve of the $p-n$ junction can be described by the classical expression with $\varepsilon \sim 2kT$. Therefore, the 'electric anomaly' is explained by the induced injection conductivity, which gives a considerable nonlinear contribution to the diode resistance.

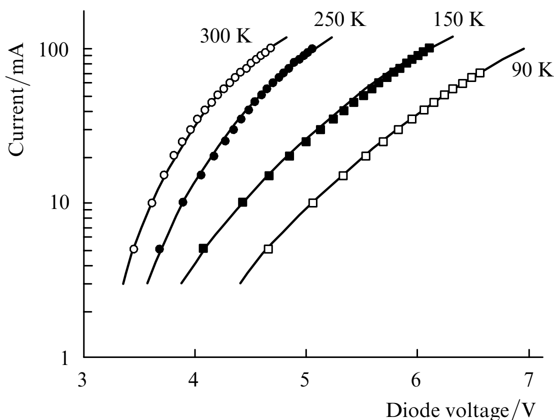

Figure 4. Experimental $I-V$ curves of the UV-emitting structure with five quantum wells (circles and squares) and calculated curves in the model taking into account the injection-induced conductivity at different temperatures.

Table 2. Fitting parameters to the curves in Fig. 4.

T/K	ε/meV	R_s/Ω	R_0/Ω	I_0/mA	ε^*/meV
300	51	6.9	42	16	203
250	42.5	7.1	60	15	350
150	25.5	9.5	145	12	530
90	15.3	11	190	11	620

Note. Values of ε^* are obtained by neglecting the injection-induced conductivity.

In some studies of nitride-based diodes, the current component with $n \approx 2$ was observed. It seems that this takes place in the cases when this component can be reliably separated from the diode voltage. In [14], $I-V$ curves were studied and it was shown that, when the bias was small ($V < 2$ V), the imperfection factor was close to two ($n = 2.28$ at 293 K), whereas for 2V $< V < 3$ V, ε is much greater than $2kT$ and changes from 140 meV at 293 K to 300 meV at 473 K. This dependence, obtained above room temperature, is opposite in sign to that discussed in this paper. The $I-V$ curve of homoepitaxial InGaN/GaN LEDs (on the GaN substrate) are presented in [15]. Here, in the case of a small bias ($V < 2$ V), tunnelling with a large value of ε (up to 1.3 eV) dominated, but in the range from 2 to 3 V, the dominating current component with $\varepsilon \approx 2kT$ was found. For one of the samples, it was found that $n = 1.9 \pm 0.9$ in the temperature range between 90 and 300 K.

It was pointed out in a number of papers that the non-ideality factor for diodes based on semiconductor nitrides was systematically large. For example, the value $n \sim 6.9$ was obtained for the p^+-n-n^+- GaN diode at 300 K and the current density $10^{-5} - 1.3$ A cm^{-2}. This concerns the region where tunnelling can be important, whereas we considered higher current densities. In [16], it was found that $n = 3.2 - 7.4$ for commercial GaN diodes. The authors of [16] explained such a large value of n by the summation of non-ideality factors at all the series junctions, including isotype ones, where the electric nonlinearity is possible. Indeed, the presence of successive nonlinear barriers is one of the reason for increasing n; however, the value $n \sim 80$ cannot be explained by this reason only.

5. Conclusions

The UV-emitting heterostructures considered in this paper are an example of the structures with strong anomalous properties. The low-temperature quenching of electroluminescence has been observed in different quantum-well InGaN-based structures, in particular, in visible LEDs. However, in our case this quenching is especially strong: at low temperature, almost no emission is observed from the quantum well, while the remaining blue emission is caused by radiative recombination in the p region. The fact that electrons are injected to the p side was taken into account in the $I-V$ curve analysis. The consideration of the injection-induced conductivity allowed us to explain the $I-V$ curve anomalies. We have analysed $I-V$ curves at room temperature by different methods, which provide satisfactory fitting in the range 5–100 mA (3.5–6.5 V). One of the methods, neglecting the injection-induced conductivity, leads to the formally strong $I-V$ curve non-ideality ($n = 8$) and other anomalies. This approach, which we used in [7], includes the injection-induced conductivity into the nonlinear conductivity of the $p-n$ junction, which causes the formal anomaly. Here, we reconsidered and refined this approach by separating the injection-induced conductivity according to the model proposed.

Figure 2 shows the $I-V$ curve fitting taking into account the induced conductivity calculated according to the 'quasi-equilibrium' model of the electron distribution in

the quantum well and in the p-AlGaN region. It is difficult to extend this model to low temperatures because we assume that the capture of electrons in the quantum well slows down and the well population does not correspond to the Fermi quasi-level in the p emitter. A more flexible model of the induced conductivity was used in the temperature range from 90 to 300 K. The results of calculations are shown in Fig. 4 where the fittings of $I-V$ curves at 300 K are presented. This model postulates that the concentration of excess carriers in emitter layers is described by a simple (in these calculations, power) function of the pump current. Note once more that a new interpretation does not require the assumption of the tunnelling injection because the question about the non-ideality of the $I-V$ curve for the $p-n$ junction is eliminated.

These anomalies are also manifested to a different extent in other devices based on large-gap semiconductors as well as in IR radiation sources and laser diodes. It was found already in 1984 that threshold anomalies in some GaAs lasers are caused by the fact that the leakage of carriers to emitter regions leads to a nonlinear change in the resistance of passive regions [17]. We assume that because this effect of the induced conductivity outside the active region indicates to a significant leakage of injected carriers and to a noticeable voltage drop in passive regions, the optimisation of the emitting structures for obtaining regular $I-V$ curves (i.e., without the anomalies described above) will improve simultaneously the recombination balance, resulting in a higher efficiency of the emitting structures.

Acknowledgements. This work was partially supported by the Federal programs 'Integration' and 'Leading Scientific Schools'. The authors thank the staff members of VEECO, NJ for their help in the preparation of UV samples.

References

1. Nakamura S., Mukai T., Senoh M. *J. Appl. Phys.*, **76** (12), 8189 (1994).
2. Nakamura S., Mukai T., Senoh M. *Appl. Phys. Lett.*, **64** (13), 1687 (1994).
3. Nakamura S., Senoh M., Iwasa N., Nagahama S. *Jpn. J. Appl. Phys.*, **34**, L797 (1995).
4. Nakamura S., Senoh M., Nagahama S., Iwasa N., Yamada T., Matsushita T., Kiyoku H., Sugimoto Y. *Jpn. J. Appl. Phys.*, **35** (1B), Pt. 2, L 74 (1996).
5. Eliseev P.G., Osinski M., Li H., Akimova I.V. *Appl. Phys. Lett.*, **75** (24), 3838 (1999).
6. Pope I.A., Smowton P.M., Blood P., Thomson J.D., Kappers M.J., Humpreys C.J. *Appl. Phys. Lett.*, **82** (17), 2755 (2003).
7. Lee J., Eliseev P.G., Osinski M., Lee D.-S., Florescu D.I, Guo S., Pophristic M. *IEEE J. Select. Topics Quantum Electron.*, **9** (5), 1239 (2003).
8. Amano H., Kito M., Hiramatsu K., Akasaki I. *J. Lumin.*, **48/49**, 666 (1991).
9. Dumin D.J., Pearson G.L. *J. Appl. Phys.*, **36** (11), 3418 (1965).
10. Wang J., Kim K.W., Littlejohn M.A. *Appl. Phys. Lett.*, **71** (6), 820 (1997).
11. Domen K., Soejima R., Kuramata A., Tanahashi T. *MRS Internet J. Nitride Semicond. Res.*, **3**, 2 (1998).
12. Shockley W. *Bell Syst. Techn. J.*, **35**, 1 (1956).
13. Kazarinov R.F., Pinto M.R. *IEEE J. Quantum Electron.*, **30** (1), 49 (1994).
14. Chitnis A., Kumar A., Shatalov M., Adivarahan V., Lunev A., Wang J.W., Simin G., Asif Khan M., Gaska R, Shur M. *Appl. Phys. Lett.*, **77** (23), 3800 (2000).
15. Franssen G., Litwin-Staszewska E., Piotrowski R., Suski T., Perlin P. *J. Appl. Phys.*, **94** (9), 6122 (2003).
16. Shah J.M., Li Y.-L., Gessmann T., Schubert E.F. *J. Appl. Phys.*, **94** (4), 2627 (2003).
17. Eliseev P.G., Okhotnikov O.G., Pak G.T. *Kratk. Soobshch. Fiz. FIAN*, (3), 21 (1984).